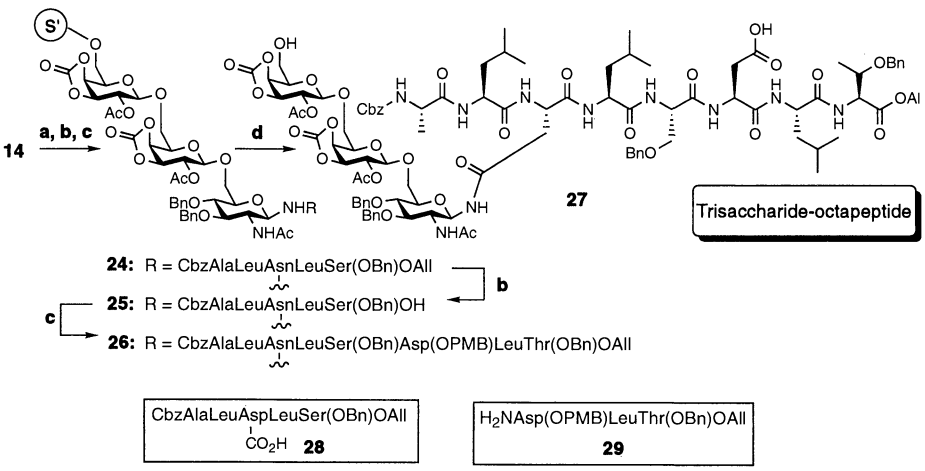

Scheme 4. Extension of the peptide portion of the glycopeptide on the solid support. PMB = *p*-methoxybenzyl. [**a**] **28**, IIDQ, and CH_2Cl_2 (**14** → **24**); [**b**] $Pd(PPh_3)_4$, dimethylbarbituric acid, and THF; [**c**] **29**, IIDQ, and CH_2Cl_2; [**d**] HF·pyridine, anisole, and CH_2Cl_2 (**26** → **27**).

synthesis, one should also consider the method of Wong, which involves enzymatically mediated elaboration of a solid phase–bound glycosylated peptide construct using glycosyl transferases to append unprotected nucleoside phosphate-activated monosaccharides in the elongation phase (*21*). By this method, retrieval from the solid support is mediated by protease action. The relief from protecting groups in enzymatically mediated chemistry can be a substantial advantage. Both Wong's method and our method allow the use of unnatural amino acids and non–amino acids. The method described herein is, in principle, totally general in that it does not require the existence of the transferases and the availability of nucleoside-activated hexoses. It can also accommodate the inclusion of unnatural (artificial) sugars in the scheme. Such building blocks are available from the Lewis acid–catalyzed diene-aldehyde cyclocondensation reaction (*22*). All workable approaches, whether purely chemical or chemoenzymatic, are complementary for reaching the common goal of carefully designed, fully synthetic glycopeptides.

REFERENCES AND NOTES

1. M. J. McPherson, P. Quirke, G. R. Taylor, Eds., *PCR: A Practical Approach* (IRL Press, Oxford, UK, 1991); G. M. Blackburn and M. J. Gait, Eds., *Nucleic Acids in Chemistry and Biology* (IRL Press, Oxford, UK, 1990); A. M. Bray, A. G. Jhingran, R. M. Valerio, N. J. Maeji, *J. Org. Chem.* **59**, 2197 (1994); G. Jung and A. G. Beck-Sickinger, *Angew. Chem. Int. Ed. Engl.* **31**, 367 (1992); M. A. Gallop, R. W. Barrett, W. J. Dower, S. P. A. Fodor, E. M. Gordon, *J. Med. Chem.* **37**, 1233 (1994); H. P. Nestler, P. A. Bartlett, W. C. Still, *J. Org. Chem.* **59**, 4723 (1994).
2. M. Meldal, *Curr. Opin. Struct. Biol.* **4**, 710 (1994).
3. T. Feizi and D. Bundle, *ibid.*, p. 673.
4. O. P. Bahl, in *Glycoconjugates: Composition, Structure, and Function*, H. J. Allen and E. C. Kisailus, Eds. (Dekker, New York, 1992), p. 1–12.
5. A. Kobata, *Acc. Chem. Res.* **26**, 319 (1993).
6. G. Opdenakker, P. M. Rudd, C. P. Ponting, R. A. Dwek, *FASEB J.* **7**, 1330 (1993).
7. A. Dell and K.-H. Khoo, *Curr. Opin. Struct. Biol.* **3**, 687 (1993).
8. R. A. Dwek, C. J. Edge, D. J. Harvey, M. R. Wormald, R. B. Parekh, *Annu. Rev. Biochem.* **62**, 65 (1993).
9. Y. C. Lee and R. T. Lee, Eds., *Neoglycoconjugates: Preparation and Applications* (Academic Press, London, 1994).
10. E. Watson, A. Bhide, H. van Halbeek, *Glycobiology* **4**, 227 (1994).
11. M. A. Lehrman and Z. Yucheng, U.S. Patent 5 272 070 A (1993).
12. M. Meldal, in (*9*), p. 145; S. J. Danishefsky and J. Y. Roberge, in *Glycopeptides and Related Compounds: Chemical Synthesis, Analysis and Applications*, D. G. Large and C. D. Warren, Eds. (Dekker, New York, in press).
13. S. T. Cohen-Anisfeld and P. T. Lansbury Jr., *J. Am. Chem. Soc.* **115**, 10531 (1993).
14. S. T. Anisfeld and P. T. Lansbury Jr., *J. Org. Chem.* **55**, 5560 (1990).
15. D. Vetter, D. Tumelty, S. K. Singh, M. A. Gallop, *Angew. Chem. Int. Ed. Engl.* **34**, 60 (1995).
16. J. T. Randolph, K. F. McClure, S. J. Danishefsky, *J. Am. Chem. Soc.*, in press; J. T. Randolph and S. J. Danishefsky, *Angew. Chem. Int. Ed. Engl.* **33**, 1470 (1994); S. J. Danishefsky, J. T. Randolph, J. Y. Roberge, K. F. McClure, R. B. Ruggeri, in *The Schering Lecture Series* (Schering, Germany, 1995); *Polym. Prepr. Am. Chem. Soc. Div. Polym. Chem.* **35**, 977 (1994).
17. S. J. Danishefsky, K. F. McClure, J. T. Randolph, R. B. Ruggeri, *Science* **260**, 1307 (1993).
18. A. J. Robinson and P. B. Wyatt, *Tetrahedron* **49**, 11329 (1993).
19. F. E. McDonald and S. J. Danishefsky, *J. Org. Chem.* **57**, 7001 (1992).
20. C. Unverzagt and H. Kunz, *Bioorg. Med. Chem.* **3**, 197 (1993).
21. M. Schuster, P. Wang, J. C. Paulson, C.-H. Wong, *J. Am. Chem. Soc.* **116**, 1135 (1994).
22. S. J. Danishefsky, *Chemtracts Org. Chem.* **2**, 273 (1989); D. B. Berkowitz, S. J. Danishefsky, G. K. Schulte, *J. Am. Chem. Soc.* **114**, 4518 (1992).
23. The polymer-bound disaccharide **18** was prepared from polymer-bound galactal carbonate and 3,4-galactal carbonate according to a procedure described in (*17*).
24. R. U. Lemieux and S. Levine, *Can. J. Chem.* **42**, 1473 (1964).
25. S. Matsuura, C.-H. Niu, J. N. Cohen, *Chem. Commun.* **1976**, 451 (1976).
26. H. Kunz and J. März, *Synlett* **1992**, 591 (1992).
27. D. A. Jones Jr., *Tetrahedron Lett.* **33**, 2853 (1977).
28. H. Paulsen, M. Schultz, D. Klamann, B. Waller, M. Paal, *Liebigs. Ann. Chem.* **1985**, 2028 (1985).

29. This research was supported by NIH grant AI 16943. We also acknowledge a National Science and Engineering Research Council (Canada) postdoctoral fellowship to J.Y.R. and a NIH postdoctoral training grant T32 CA62948 to X.B.

9 February 1995; accepted 19 May 1995

Inhibitor-Enhanced Electron Transfer: Copper Cytochrome c as a Redox-Inert Probe of Ternary Complexes

Jian S. Zhou, Judith M. Nocek, Michael L. DeVan, Brian M. Hoffman*

Copper-substituted cytochrome c (CuCc) has been used as a structurally faithful, redox-inert inhibitor to probe the mechanism of electron transfer (ET) between Cc molecules and cytochrome c peroxidase (CcP). This inhibitor enhances photoinduced ET quenching of the triplet excited state of a zinc-substituted protein (ZnCcP or ZnCc) by its iron(III) partner (Fe^{3+}Cc or Fe^{3+}CcP). These results show that CcP and Cc form a ternary complex in which one Cc molecule binds tightly at a surface domain of CcP having low ET reactivity, whereas the second Cc molecule binds weakly to the 1:1 complex at a second domain with markedly greater ($\sim 10^3$) reactivity. These results also rule out the possibility that Cc bound at the second domain cooperatively enhances ET to Cc at the first domain. The multiphasic kinetics observed for the photoproduced ET intermediate do not reflect electron self-exchange between two Cc molecules within the ternary complex.

Respiration and metabolism depend on the sequential transfer of electrons from one protein to another (*1*), and this ET in turn depends on the recognition and docking, as well as the reaction, of the ET partners (*2*). Issues of binding specificity and of reactivity in protein-protein reactions are analogous to those in enzyme-substrate reactions, but studies of ET complexes have lacked paral-

Department of Chemistry, Northwestern University, 2145 Sheridan Road, Evanston, IL 60208, USA.

*To whom correspondence should be addressed.

lels to the imaginative uses of substrate analogs and inhibitors in enzymology (*3*). We demonstrate here that fundamental mechanistic questions about the reaction between protein ET partners can be resolved by the use of a metalloprotein that has been converted into an ET inhibitor through appropriate metal substitution. This strategy is illustrated by the use of Cu(II)-substituted Cc (*4*), a structurally faithful (*4, 5*) but inert analog of Fe^{2+}Cc, to probe ET within a ternary complex involving two Cc molecules and one CcP.

We have studied heme-heme ET within the Cc–CcP (*6*) complex by monitoring the ET cycle composed of (i) photoinduced ET from a Zn(II)-substituted protein, ZnCcP or ZnCc, to the corresponding partner, Fe^{3+}Cc or Fe^{3+}CcP, followed by (ii) the return of the resulting charge-transfer intermediate, $[(ZnCcP)^+, Fe^{2+}Cc]$ or $[(ZnCc)^+, Fe^{2+}CcP]$, to the ground state (*7–12*). The validity of ZnCc and ZnCcP as structurally faithful analogs of the corresponding ferrous proteins has recently been supported by the solution nuclear magnetic resonance study of ZnCc (*13*). Likewise, CuCc is structurally ideal as a competitive ET inhibitor because the incorporation of Cu(II) does not significantly perturb the structure or electrostatic properties of Fe^{2+}Cc (*4, 5*). Control experiments show that CuCc is ideal functionally because it is redox- and photoinactive and does not quench the excited state of either ZnCcP or ZnCc; quenching by energy transfer is precluded because the CuCc absorption spectrum does not overlap their emission spectra. The utility of this probe can be enhanced by using CuCc prepared with protein from multiple sources. Fungal Cc, such as that from *Pichia membranefaciens* (Pm), has a greater affinity for CcP than Cc from vertebrates (*7, 14, 15*), and either type can be prepared with a selected metal ion—Fe, Zn, or Cu. Thus, it is possible to perform an experiment in which CcP preferentially binds a fungal metallo-Cc having a selected metal and reactivity (Fe^{3+}Cc, ET quencher; ZnCc, ET photodonor; and CuCc, inhibitor) in the presence of a vertebral Cc with a different metal and a different reactivity. We describe the use of CuCc first as a competitive ET inhibitor in the study of intracomplex photoinduced ET and then in the study of the thermal return of the charge-transfer intermediate to the ground state.

Earlier observations (*7, 12, 16*) of photoinduced heme-heme ET between Cc and CcP have shown that CcP binds two Cc molecules simultaneously. This result establishes an early suggestion (*14*) and has recently received confirmation (*17*). Intriguingly, at low ionic strength the first Cc binds with a high affinity and low reactivity; the second binds with low affinity to

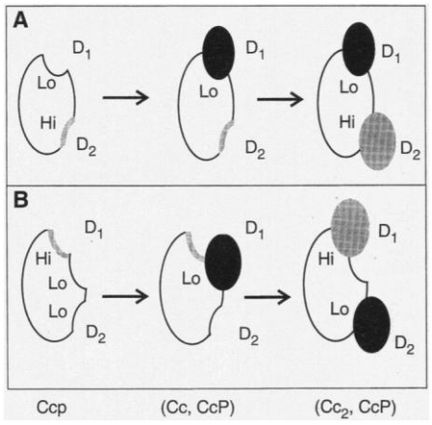

Fig. 1. Schematic representation of limiting two-domain mechanisms for ET between CcP and Cc. (**A**) Model with two independent ET domains, with D_1 having high affinity but low (Lo) reactivity and D_2 having low affinity but high (Hi) reactivity. (**B**) Model with cooperative ET. The strong binding domain on CcP, D_1, consists of two overlapping (exclusive) binding sites, one of which has high reactivity and one of which has low reactivity. The weakly binding domain on CcP, D_2, consists of a low-reactivity binding site or sites.

give a highly reactive 2:1 complex (*7*). A complete characterization of the system requires the determination of stoichiometric binding and rate constants, as well as their mechanistic interpretation. The simplest, limiting, 2:1 kinetic model would involve binding and reaction at two independent domains (each possibly with multiple overlapping sites) (Fig. 1A). However, CcP is too small to bind two Cc molecules without some interaction between them, and one must therefore consider cooperativity between the two bound Cc molecules (Fig. 1B). The first Cc might bind tightly at one site, but in a nonreactive conformation; this "tight" site could then become reactive upon the binding of a second Cc at a nonreactive, "remote" site.

The inhibitor CuCc is readily incorporated within the conventional approach of monitoring ET quenching of the ZnCcP triplet excited state, ^{3}(ZnCcP), by Fe^{3+}Cc (*7, 9, 10*). Figure 2 shows the titration of an equimolar solution of ZnCcP and horse heart Fe^{3+}Cc(H) (pH 7.0, μ = 4.5 mM; 20°C) by a solution of the CuCc(Pm) inhibitor. Before the addition of inhibitor, photoinduced ET from ^{3}(ZnCcP) to Fe^{3+}Cc(H) is manifested in quenching with a rate constant $k_q = 26\ s^{-1}$ (*18*). If this ET quenching were associated with a 1:1

$$^3ZnCcP + Fe^{3+}Cc \overset{K_1}{\rightleftarrows} {}^3ZnCcP{:}Fe^{3+}Cc \xrightarrow{k_1} (ZnCcP)^+{:}Fe^{2+}Cc \quad (1)$$

$$k_q = k_1[ZnCcP, Fe^{3+}Cc]/[ZnCcP]_0 \quad (2)$$

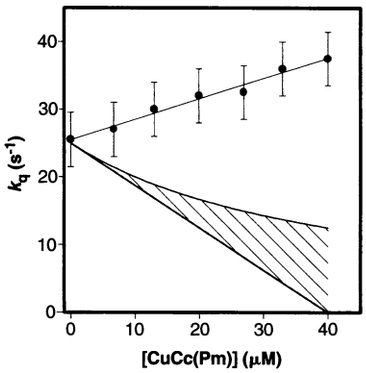

Fig. 2. The ET quenching of ^{3}(ZnCcP) by Fe^{3+}Cc(H) as a function of [CuCc(Pm)]. (Uncertainties in k_q are $\pm 4\ s^{-1}$.) The solid straight line is included to guide the eye. The shaded area represents the range of results that could be seen for 1:1 binding, with the upper boundary arising with equal affinities for Cc(H) and Cc(Pm) and the lower boundary arising when Cc(Pm) has a far higher affinity. Conditions: [ZnCcP] = $[Fe^{3+}Cc(H)]$ = 40 μM in potassium phosphate buffer (pH 7.0, μ = 4.5 mM) at 20°C.

complex as in Eq. 1, then in the rapid-exchange limit that applies here (*19*) the quenching would be described by Eq. 2. Within this model, the quenching of ^{3}ZnCcP by Fe^{3+}Cc(H) must decrease monotonically with increasing concentration of the competitive inhibitor, CuCc(Pm); because Cc(Pm) binds CcP more tightly than does Cc(H), k_q would decrease by more than a factor of 2 over the course of the titration with CuCc(Pm) (Fig. 2). Instead, the quenching is slightly enhanced with increasing concentration of the inhibitor CuCc. This result shows that the stoichiometry of the Cc–CcP complex is not 1:1 but 2:1 or higher. However, the data have not been analyzed to derive binding and ET rate constants for a 2:1 binding model because the increase in k_q with [CuCc(Pm)] is small and the titration curve is essentially linear (*20*).

We have resolved this difficulty by using CuCc in the "inverse" experiment (*12*), where the excited state of the photoactive "substrate," ZnCc(H), is quenched by ET to the Fe^{3+}CcP enzyme. Figure 3 presents the results of a titration of 10 μM ZnCc(H) (pH 7.0, μ = 4.5 mM) by the preformed 1:1 complex between Fe^{3+}CcP and the strongly binding inhibitor, CuCc(Pm). If binding to CcP involved only a 1:1 complex, quenching of the ^{3}ZnCc(H) would be inhibited in this experiment because the Fe^{3+}CcP binding domain (reactive domain) is blocked by CuCc(Pm). However, the quenching is enhanced. During the titration with the inhibitor complex [CuCc(Pm), Fe^{3+}CcP], the quenching constant increases monotonically to $k_q \sim 400\ s^{-1}$ at the end of the titration, a value far greater than the maximum observed in the titration of ZnCc(H) with

Fe^{3+}CcP alone (*21*). The titration curve is hyperbolic, signifying 1:1 binding. This result suggests that CuCc(Pm) binds so well to the strongly binding domain of Fe^{3+}CcP that we can treat the [CuCc(Pm):Fe^{3+}CcP] complex as a single species that binds one additional ZnCc(H) at a second, weakly binding domain. A fit of these data to a 1:1 binding expression (*7*) gives $K_2 = 6.5 \times 10^3$ M^{-1} as the stoichiometric association constant for the binding of the second Cc to form the 2:1 complex at $\mu = 4.5$ mM and gives $k_2 = 1530$ s^{-1} for photoinitiated ET within this complex.

The two titration experiments with the inhibitor CuCc(Pm) (Figs. 2 and 3) were designed to test for cooperative ET at the strongly binding domain in the 2:1 Cc–CcP complex (Fig. 1). In both experiments, the tight-binding domain on CcP is occupied by a redox-inert CuCc(Pm), which blocks access to this domain by a redox-active Cc(H), either ZnCc(H) (Fig. 3) or Fe^{3+}Cc(H) (Fig. 2). Thus, the enhanced ET quenching in the presence of inhibitor is inconsistent with the cooperative model of Fig. 1B, in which ET between CcP and a Cc bound at its strongly binding domain 1 is enhanced when a second Cc binds at nonreactive domain 2. The experiments instead indicate that the strongly binding domain of CcP has low reactivity; one may provisionally assign to this domain the quenching constant previously reported for the 1:1 complex, $k_1 \sim 5$ s^{-1} (*12*, *16*). The ET rate constant obtained from the fitting of the titration data in Fig. 3 ($k_2 \sim 1530$ s^{-1}) is associated with the weakly binding domain within the 2:1 Cc–CcP complex.

The CuCc inhibitor also has been used to probe the mechanism of the Fe^{2+}Cc $\rightarrow$ $(ZnCcP)^+$ thermal ET within the $[(ZnCcP)^+, Fe^{2+}Cc]$ ET intermediate produced by photoinduced ET. It has been reported that this reaction displays multiphasic, intracomplex kinetics (*7*, *9*), and this behavior has been provisionally interpreted in terms of gating by conformational interconversion (*22*). The discovery that photoinitiated ET occurs primarily within a 2:1 complex means that the ET intermediate actually has the 2:1 stoichiometry $[(ZnCcP)^+, Fe^{2+}Cc, Fe^{3+}Cc]$. This, in turn, raises the possibility that the multiphasic kinetics displayed by this intermediate reflect enhanced electron self-exchange (*23*) between Fe^{2+}Cc and Fe^{3+}Cc on the surface of ZnCcP, before the reduction of the $(ZnCcP)^+$. We have tested this possibility by photolysis of ZnCcP solutions that contain comparable concentrations of both the redox-active Fe^{3+}Cc(H) and the strongly binding inhibitor CuCc(Pm), a situation that corresponds to the early phases in the titration of Fig. 2. In this experiment the strongly binding domain is occupied by the CuCc(Pm) inhibitor, and this would eliminate self-exchange ET within the ET intermediate and simplify the kinetic progress curve if this process were contributing.

Logarithmically plotted kinetic progress curves for the $[(ZnCcP)^+, Fe^{2+}Cc]$ charge-transfer species in the absence (Fig. 4A) and presence (Fig. 4B) of CuCc(Pm) indicate that neither trace can be described by a single kinetic phase, as would be the case if the intermediate were formed according to Eq. 1 and returned to the ground state by first-order, intracomplex ET. Instead, each trace can only be described with a function that is the sum of at least three kinetic phases (*9*). Furthermore, fits of the two traces to a three-phase function (*24*) give for each essentially the same set of thermal ET rate constants and only slight differences in the weights of the phases (see Fig. 4). The small but noticeable differences in the shapes of the curves do not reflect significant changes in the ET return reaction but rather are largely brought about by the enhancement of photoinduced ET caused by the presence of the inhibitor, as in Fig. 2. Because the charge-transfer intermediate being observed in the presence of inhibitor has the preponderant stoichiometry $[(ZnP)^+CcP, CuCc, Fe^{2+}Cc]$, the kinetics of the intermediate clearly are not controlled by self-exchange ET between two Cc molecules on the CcP surface.

The use of CuCc as an ET inhibitor thus rules out both the hypothesis of cooperative photoinitiated ET within the 2:1 complex (Fig. 1) and that of intracomplex self-exchange within the ET intermediate. The simplest kinetic scheme that is consistent with current data (Fig. 1A) involves sequential binding, where the first Cc binds strongly at a nonreactive domain and the second binds weakly at a reactive one, with the observed ET largely occurring in the 2:1 species. The fit of the titration curve of Fig. 3 based on the use of this model gives values for the affinity of a second Cc for the 1:1 Cc–CcP complex (K_2) at $\mu = 4.5$ mM as well as for the ET rate constant at the low-affinity domain (k_2) in the 2:1 Cc–CcP complex, thereby quantifying a picture of binding at two distinct surface domains of CcP with reactivities for heme-heme ET that differ by roughly 10^3. Given current estimates, for the average distance-decay of ET rates in proteins (*25*, *26*), such a rate ratio translates into a difference in ET distances for the two domains of ~5 Å. It may be that the domain seen here to have poor heme-heme reactivity is more effective in reduction of the tryptophan radical of CcP oxidized by hydrogen peroxide (compound ES) (*27*, *28*).

The strategy developed here can be extended to the study of ET involving both other hemoproteins and more complicated systems such as the photosynthetic reaction center (*29*) and cytochrome oxidase and to the investigation of ET involving nonheme proteins (such as plastocyanin and azurin) (*30*) that are susceptible to substitution with redox-inactive metal ions (*31*).

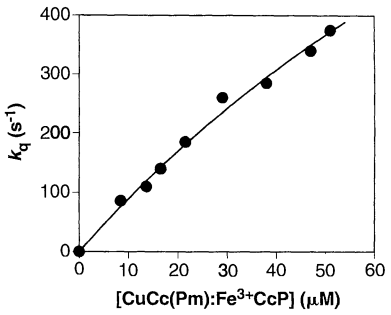

Fig. 3. Quenching titration of ^{3}ZnCc(H) by the inhibitor complex [CuCc(Pm), Fe^{3+}CcP]. The solid line is a fit to a 1:1 binding isotherm (*7*) with $K_2 = 6.5 \times 10^3$ M^{-1} and $k_2 = 1530$ s^{-1}. Conditions: [ZnCc(H)] = 10 μM in potassium phosphate buffer (pH 7.0, $\mu = 4.5$ mM) at 20°C.

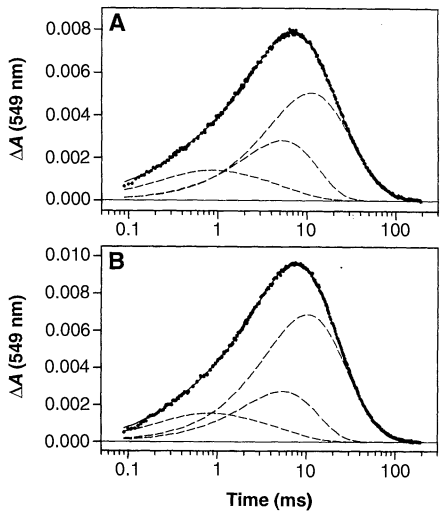

Fig. 4. Kinetic progress curves for the ET intermediate for (**A**) 0 μm and (**B**) 20 μM CuCc(Pm). Conditions: [ZnCcP] = 20 μM and [Fe^{3+}Cc(H)] = 36 μM in potassium phosphate buffer (pH 7.0, μ = 4.5 mM) at 20°C and wavelength $\lambda = 549$ nm. The solid lines are the theoretical fits obtained with the multiexponential function described in (*24*), using the following parameters: (A) $k_1 = 3833$ s^{-1}, $f_1 = 0.69$, $k_2 = 206$ s^{-1}, $f_2 = 0.16$, $k_3 = 39$ s^{-1}, $f_3 = 0.15$, $k_{obs} = 173$ s^{-1}, and $\beta = 9.0$; (B) $k_1 = 4000$ s^{-1}, $f_1 = 0.68$, $k_2 = 190$ s^{-1}, $f_2 = 0.13$, $k_3 = 45$ s^{-1}, $f_3 = 0.19$, $k_{obs} = 180$ s^{-1}, and $\beta = 10.4$. The dashed lines show the contribution of the individual kinetic phases to the observed signals.

REFERENCES AND NOTES

1. Y. Hatefi, *Annu. Rev. Biochem.* **54**, 1015 (1985).
2. M. J. Clarke *et al.*, Eds., *Struct. Bonding (Berlin)* **75** (1991); H. Sigel and A. Sigel, Eds., *Met. Ions Biol. Syst.* **27** (1991).

3. R. B. Silverman, *Mechanism-Based Enzyme Inactivation: Chemistry and Enzymology* (CRC Press, Boca Raton, FL, 1988).
4. M. C. Findlay, L. C. Dickinson, J. C. W. Chien, *J. Am. Chem. Soc.* **99**, 5168 (1977).
5. G. Moore *et al.*, *J. Inorg. Biochem.* **12**, 1 (1980).
6. Preparative procedures have been described: ZnCcP (*7–10*), ZnCc (*11*), and CuCc (*4*). The ET kinetics were performed by laser flash kinetic spectrophotometry (*7–10*) with the 532-nm output of a Q-switched Nd:yttrium-aluminum-garnet laser under anaerobic conditions at pH 7.0 and 20° ± 0.2°C. The transient absorption apparatus has a transient digitizer (LeCroy) that collects 50,000 data points so that the full progress curve of the intermediate could be collected in a single trace. Before analysis, data were compressed logarithmically. The decays of the ^{3}ZnCcP and ^{3}ZnCc were monitored at 475 nm and 460 nm, respectively. The formation and decay of the resulting charge-transfer intermediate, [(ZnCcP)$^+$, Fe^{2+}Cc], was monitored at a wavelength of 549 nm, the isosbestic point for the ^{3}ZnCcP-ZnCcP absorbance.
7. E. D. A. Stemp and B. M. Hoffman, *Biochemistry* **32**, 10848 (1993).
8. B. M. Hoffman, M. J. Natan, J. M. Nocek, S. A. Wallin, *Struct. Bonding (Berlin)* **75**, 85 (1991).
9. S. A. Wallin *et al.*, *J. Am. Chem. Soc.* **113**, 1842 (1991).
10. J. M. Nocek *et al.*, *ibid.*, p. 6822.
11. J. M. Vanderkooi and M. Erecinska, *Eur. J. Biochem.* **60**, 199 (1975); *ibid.* **64**, 381 (1976).
12. J. S. Zhou and B. M. Hoffman, *J. Am. Chem. Soc.* **115**, 11008 (1993).
13. H. Anni, J. M. Vanderkooi, L. Mayne, *Biochemistry* **34**, 5744 (1995).
14. C. H. Kang, S. Ferguson-Miller, E. Margoliash, *J. Biol. Chem.* **252**, 919 (1977).
15. G. McLendon *et al.*, *J. Am. Chem. Soc.* **115**, 3665 (1993); Q. Zhang *et al.*, *Mol. Cryst. Liq. Cryst.* **199**, 343 (1991).
16. J. S. Zhou and B. M. Hoffman, *Science* **265**, 1693 (1994).
17. M. R. Mauk, J. C. Ferrer, A. G. Mauk, *Biochemistry* **33**, 12609 (1994).
18. The quenching rate constant (k_q) is the difference between the observed (k_{obs}) and the intrinsic (k_D) decay rate constant of ^{3}(ZnCcP).
19. The decay of the ^{3}(ZnCcP) is exponential in the absence and presence of Fe^{3+}Cc. We have ruled out the possibility of a very fast ET process from ^{3}(ZnCcP) to Fe^{3+}Cc by monitoring triplet decay on the microsecond and nanosecond time scales and by observing the lack of an effect of the quencher on the change in the absorbance (ΔA) of ^{3}(ZnCcP) at time zero. This exponential decay behavior of ^{3}ZnCcP indicates that the ET quenching process is in the rapid-exchange limit, that is, the intracomplex ET rate constant is much slower than the complex dissociation rate constant.
20. The effects increase with increasing protein concentrations, but high optical absorbance precludes the use of still higher concentrations.
21. In fact, a quenching titration of ZnCc with Fe^{3+}CcP under these conditions displayed a maximum of k_q = 25 s^{-1} at a concentration ratio of [ZnCc] to [Fe^{3+}CcP] = 2:1; the quenching rate constant decreased with further addition of the quencher Fe^{3+}CcP (*12*).
22. B. M. Hoffman and M. A. Ratner, *J. Am. Chem. Soc.* **109**, 6237 (1987).
23. D. W. Dixon, X. Hong, S. E. Woehler, *Biophys. J.* **56**, 339 (1989).
24. At this point, we are concerned not with the uniqueness of this description but rather with the complexity of the time course. The function explored here is

$$\Delta A = \beta\Sigma\{f_i[\exp(-k_{obs}t) - \exp(-k_it)]/(k_i - k_{obs})\}$$

where k_{obs} is the triplet decay constant, k_i is the thermal back-ET rate constant of phase i, and Σf_i = 1. We are preparing a mechanistic analysis of curves such as those in Fig. 3 (J. S. Zhou, J. M. Nocek, M. L. DeVan, B. M. Hoffman, unpublished results).
25. D. N. Beratan, J. N. Onuchic, J. R. Winkler, H. B. Gray, *Science* **258**, 1740 (1992).
26. C. C. Moser, J. M. Keske, K. Warncke, R. S. Farid, P. L. Dutton, *Nature* **355**, 796 (1992).
27. R. Q. Liu, S. Hahm, M. Miller, B. Durham, F. Millet, *Biochemistry* **34**, 973 (1995).
28. H. Pelletier and J. Kraut, *Science* **258**, 1748 (1992).
29. Indeed, it has been reported that Cc binds to the reaction center at two sites, much as reported here [C. C. Moser and P. L. Dutton, *Biochemistry* **27**, 2450 (1988)].
30. J. S. Zhou and N. M. Kostić, *J. Am. Chem. Soc.* **115**, 10796 (1993); L. Qin and N. M. Kostić, *Biochemistry* **32**, 6073 (1992); I. J. Chang, H. B. Gray, J. R. Winkler, *J. Am. Chem. Soc.* **113**, 7056 (1991).
31. W. B. Church, J. M. Guss, J. J. Potter, H. C. Freeman, *J. Biol. Chem.* **261**, 234 (1986); H. R. R. Engeseth, D. R. McMillin, J. D. Otvos, *ibid.* **259**, 4822 (1984); L. M. Utschig, J. G. Wright, T. V. O'Halloran, *Methods Enzymol.* **226**, 71 (1993).

32. This research was supported under National Institutes of Health grant HL13531.

21 February 1995; accepted 22 May 1995

Experimental Studies and Theoretical Predictions for the H + D_2 → HD + D Reaction

L. Schnieder,* K. Seekamp-Rahn, J. Borkowski, E. Wrede, K. H. Welge, F. J. Aoiz, L. Bañares, M. J. D'Mello, V. J. Herrero, V. Sáez Rábanos, R. E. Wyatt

The H + H_2 exchange reaction constitutes an excellent benchmark with which to test dynamical theories against experiments. The H + D_2 (vibrational quantum number v = 0, rotational quantum number j = 0) reaction has been studied in crossed molecular beams at a collision energy of 1.28 electron volts, with the use of the technique of Rydberg atom time-of-flight spectroscopy. The experimental resolution achieved permits the determination of fully rovibrational state–resolved differential cross sections. The high-resolution data allow a detailed assessment of the applicability and quality of quasi-classical trajectory (QCT) and quantum mechanical (QM) calculations. The experimental results are in excellent agreement with the QM results and in slightly worse agreement with the QCT results. This theoretical reproduction of the experimental data was achieved without explicit consideration of geometric phase effects.

The H + H_2 exchange reaction has been the prototype in the realm of reaction dynamics since the first studies in the field. A good survey of work up to 1990 can be found in (*1*). Particularly intense activity has taken place during the last decade. Great improvements in the quantum dynamical methodology (*2–7*) together with the introduction of laser techniques (*1*) have produced a large amount of new data in a short time, and this rapid progress has not always been free of controversy. The long discrepancy between experiment and theory about the value of the rate constant for the D + H_2 (v = 1) reaction (*1*), the dispute about the possible observation of dynamical resonances in the integral cross section (*1–3, 8, 9*) (finally settled against this possibility), and the tentative assignment of features in the differential cross section to broad QM resonances (*10*), which were later also obtained in a QCT calculation (*11*), are examples of such controversies.

Zare and co-workers (*12–14*) have recently measured rotationally state-specific integral cross sections and rate constants for the D + H_2 (v = 1) → HD (v', j') + H reaction. In a first experiment, they generated D atoms by photolyzing DBr and used resonance-enhanced multiphoton ionization to detect the HD molecules. Noticeable discrepancies were found between the experimental results and several accurate QM (*15*) and QCT (*15*) calculations on different ab initio potential energy surfaces (PESs) (*16, 17*). Further experiments were carried out with DI (*13, 14*), after some experimental problems were detected with the DBr precursor. These measurements were in much better agreement with QCT results (*18*), and especially with new QM calculations (*14*). However, some discrepancies persisted between experiment and theory; these were tentatively attributed to failures in the PES (*14*).

Most theoretical calculations have been carried out on the lowest lying Born-Oppenheimer PES of H_3. In recent works, Kuppermann and Wu (*7*) have shown that a geo-

L. Schnieder, K. Seekamp-Rahn, J. Borkowski, E. Wrede, K. H. Welge, Fakultät für Physik, Universität Bielefeld, Postfach 100131, 33501 Bielefeld, Germany.
F. J. Aoiz and L. Bañares, Departamento de Química Física, Facultad de Química, Universidad Complutense, 28040 Madrid, Spain.
M. J. D'Mello, 4155 National Center for Supercomputing Application, Beckman Institute, 405 North Mathew Avenue, Urbana, IL 61801, USA.
V. J. Herrero, Instituto de Estructura de la Materia, Consejo Superior de Investigaciones Cientificas, Serrano 123, 28006 Madrid, Spain.
V. Sáez Rábanos, Departamento de Química General y Bioquímica, ETS Ingenieros de Montes, Universidad Politécnica, 28040 Madrid, Spain.
R. E. Wyatt, Department of Chemistry and Biochemistry, University of Texas, Austin, TX 78712, USA.

*To whom correspondence should be addressed.